

Short Communication

## Simple and Facile Synthesis W-doped VO<sub>2</sub> (M) Powder Based on Hydrothermal Pathway

Chengxi Zhang<sup>1,2</sup>, Jiang Cheng<sup>2</sup>, Jin Zhang<sup>2,3</sup>, Xin Yang<sup>2,3,\*</sup>

<sup>1</sup> College of Materials Science and Engineering, Chongqing university of technology, Chongqing 400054, China

<sup>2</sup> Research Institute for New Materials Technology, Chongqing University of Arts and Sciences, Chongqing 404100, China

<sup>3</sup> Chongqing Key Laboratory of Environmental Materials and Remediation Technologies, Chongqing University of Arts and Sciences, Chongqing 404100, China

\*E-mail: [oyangx2003o@qq.com](mailto:oyangx2003o@qq.com)

Received: 12 March 2015 / Accepted: 30 April 2015 / Published: 27 May 2015

---

The present study provides a simple and facile pathway to obtain undoped and W-doped VO<sub>2</sub> (M) powder by utilizing the inexpensive and low toxic NH<sub>4</sub>VO<sub>3</sub> precursor with an economical and environmental friendly method. The XRD patterns exhibited that the W-doped VO<sub>2</sub> powder was monoclinic phase, and W atom doping almost had no influence on the crystal structure of VO<sub>2</sub> lattice. The grain size of W-doped VO<sub>2</sub> particles decreased as W atom concentration increasing. SEM images showed that particles with 1~2 microns diameter of W-doped VO<sub>2</sub> (B) were obtained by hydrothermal synthesis directly. VO<sub>2</sub> (B) transformed to VO<sub>2</sub> (M) after annealed at 750 °C in nitrogen atmosphere.

---

**Keywords:** W-doped; VO<sub>2</sub> powder; hydrothermal method

### 1. INTRODUCTION

Vanadium dioxide (VO<sub>2</sub>) has intrigued researchers for five decades since the first discovery of the existence of thermochromic properties [1, 2]. Monoclinic VO<sub>2</sub> (M) has a reversible metal-semiconductor phase transition (MST) property at about 68 °C, and its unit cell distorts during the MST transition, accompanied by a reversible switch in optical transmittance and reflectance in the infrared range. Above the phase transition temperature, it has a tetragonal lattice with the P4<sub>2</sub>/mnm rutile space group (R phase), which is reflective to infrared light; however, it shows a monoclinic structure with the P21/c space group (M phase) below the phase transition temperature, which is transparent to infrared light. On its own, VO<sub>2</sub> is important for many applications of its phase transition,

including electrochemical devices as a cathode[3, 4], smart windows[5, 6], optical switching devices[7], optical storage devices[8], etc.

A number of strategies have been employed to produce undoped or doped VO<sub>2</sub> thin films, such as sputtering[9], sol-gel methods[10], chemical vapor deposition[11], pulsed laser deposition[12] and spray pyrolysis[13]. These methods are capable of producing VO<sub>2</sub> films with various thermochromic properties. Unfortunately, the low visible light transmittance, weak optical contrast in the IR region and high metal-insulator phase transition are three main issues must be addressed, if VO<sub>2</sub> is to be used in applications like smart windows. Compared with thin films, powder can overcome such shortcomings and work more effectively, and the cost is inexpensive. Furthermore, the powder can remarkably lessen the stress for the phase change; offer the possibility of obtaining a sharper and more reproducible transition. There were also several methods that have been reported on the preparation of VO<sub>2</sub> powder, such as spray pyrolysis [14] and hydrothermal synthesis[15, 16]. For the hydrothermal synthesis, most of the studies [17, 18] used V<sub>2</sub>O<sub>5</sub> as a reactant, which exhibited a toxic property, thus limited the usage and development of this method.

In this work, we highlighted an available and facile way to synthesize high-quality W-doped monoclinic VO<sub>2</sub> (M) powder with inexpensive and low toxic NH<sub>4</sub>VO<sub>3</sub> precursor. This reaction is not limited to just VO<sub>2</sub>, but could be extended to other vanadium oxides to manipulate the composition of powder.

## 2. EXPERIMENTAL

### 2.1. Synthesis of undoped or W-doped VO<sub>2</sub> powder

Ammonium metavanadate (NH<sub>4</sub>VO<sub>3</sub>, ChengDu Kelong Chemical Co., Ltd.) and tungsten dichloride dioxide (WO<sub>2</sub>Cl<sub>2</sub>, Sinopharm Chemical Reagent Co. Ltd) were used as vanadium and tungstate source, respectively. Certain amount oxalic acid (ChengDu Kelong Chemical Co., Ltd.) was added to 10 ml NH<sub>4</sub>VO<sub>3</sub> aqueous solution containing 0.10 mol vanadium with strong stirring. Then diluted H<sub>2</sub>SO<sub>4</sub> was added dropwise to the above solution, until the pH reached ~2.5. The resulting solution was introduced into a Teflon-lined stainless steel autoclave and maintained at 180 °C for 48 hours. After air-cooling to room temperature, the dark blue precipitates were collected by centrifuging. The powder was washed with deionized water and alcohol for three times, and then dried in a vacuum oven at 70 °C for 8 h. At last, VO<sub>2</sub> powder was annealed at 750 °C in nitrogen atmosphere for 2 h.

For the preparation of W-doped VO<sub>2</sub>, the different stoichiometric volume of aqueous tungsten dichloride dioxide solution was added into the NH<sub>4</sub>VO<sub>3</sub> solution before H<sub>2</sub>C<sub>2</sub>O<sub>4</sub> was added. The W content in VO<sub>2</sub> sample could be controlled by changing tungsten concentration in precursor; other processes were the same as synthesis of VO<sub>2</sub> powder.

### 2.2. Characterization

X-ray diffraction (XRD) analysis was conducted on XRD diffractometer (TD-3500, Dandong Tongda, Ltd) at 0.4° per second with 2θ ranging from 10° to 70°, using Cu Kα1 radiation (λ=0.154056

nm). Morphologies of prepared particles were observed by scanning electron microscopy (FEI Quanta 250, USA) at an acceleration voltage of 10 KV.

### 3. RESULTS AND DISCUSSION

#### 3.1 Synthesis of $\text{VO}_2$ (M) powder

X-ray diffraction was used to check the powder structures. All peaks are indexed to  $\text{VO}_2$  (B) (JCPDS no. 81-2392, C2/m,  $a = 1.209$  nm,  $b = 0.370$  nm,  $c = 0.643$  nm) from Fig. 1. While Fig.1b diffraction peaks are indexed to JCPDS 72-0514, indicating the formation of monoclinic  $\text{VO}_2$  (M), after annealing at  $750^\circ\text{C}$  for 2h under nitrogen atmosphere, which is in accordance with other reports [19, 20]. No other phase or impurities are observed in  $\text{VO}_2$  (M) powder, and the  $\text{VO}_2$  phase transformation temperature in our sample was  $69.9^\circ\text{C}$ .

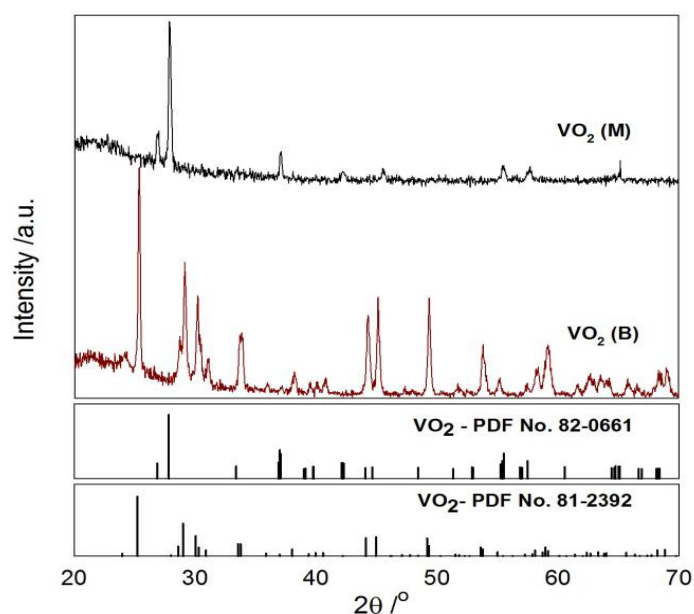


**Figure 1.** XRD patterns of prepared  $\text{VO}_2$  samples: (a)  $\text{VO}_2$  (B) powder (red line) and (b)  $\text{VO}_2$  (M) powder (blue line).

SEM images of pure  $\text{VO}_2$  (B) and  $\text{VO}_2$  (M) are shown in Fig. 2a and Fig. 2b. The microstructure of  $\text{VO}_2$  (B) phase presents needle-like structure;  $\text{VO}_2$  (M) powder that was annealed at a relatively higher temperature ( $750^\circ\text{C}$ ) shows better crystallinity and conductivity. According to the SEM image,  $\text{VO}_2$  (M) particles with a diameter about 1~2 microns, closed to the calculated grain size from X-ray diffraction results by using Debye-Scherrer formula[21]. Interestingly, the  $\text{VO}_2$  (B) powder after being annealed presents granular shape. Such a result is in coincidence with the grain growth mechanism, and the powder experienced a series of morphological changes because of the subsequent annealing.

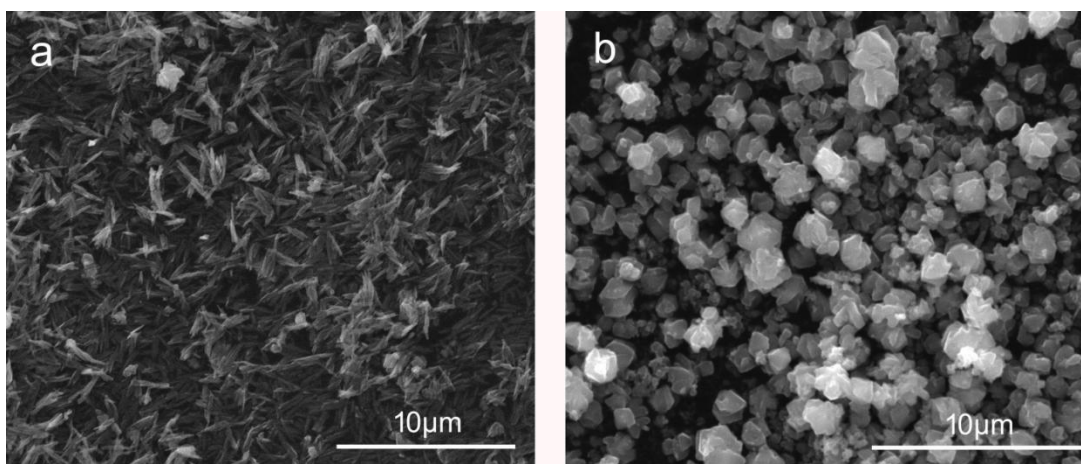


**Figure 2.** SEM images of the as-received VO<sub>2</sub> samples: (a) VO<sub>2</sub> (B) powder and (b) VO<sub>2</sub> (M) powder.

### 3.2. Synthesis of W-Doped VO<sub>2</sub> (M) powder

X-ray diffraction patterns displayed in Fig. 3 (a) exhibit two main characteristic diffraction peaks, (110) and (002), which are assignable to the VO<sub>2</sub>(B) for all doped samples (JCPDS 81-2392). Booth et al.[22] suggested that doping element could induce a local structural distortion, which restrained the grain growth of VO<sub>2</sub>. The magnified XRD pattern around (110) peak are displayed in Fig. 3b. We find that (110) peak shifts toward small reflection angle, from 25.5° to 25.3°, when W atomic concentration increases from 0.5% to 5%. So the interplanar distance (d-value) increases lightly according to Bragg's law, which may be attributed to the larger tungsten atom size than vanadium atom[23].

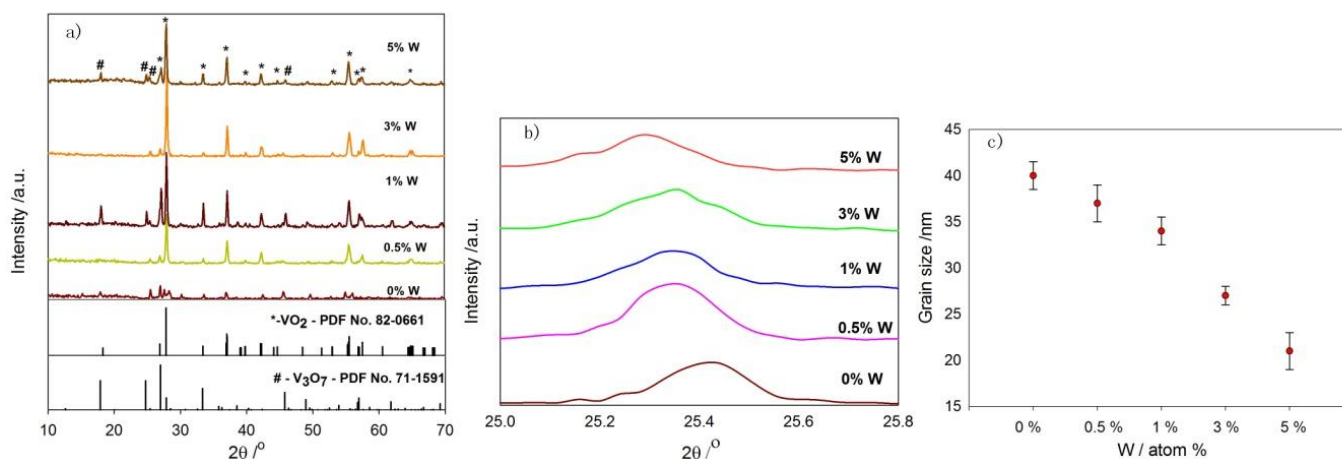


**Figure 3.** (a) The XRD patterns of obtained W-doped VO<sub>2</sub> (B) powder, (b) (110) peak of W-doped VO<sub>2</sub> (B) powder and (c) The plot of grain size as function of W concentration for W-doped VO<sub>2</sub> (B) powder.

Thermal treatment of VO<sub>2</sub> (B) powder leads to the formation of monoclinic phase (M-phase) VO<sub>2</sub> with a preferred orientation of (011)<sub>M</sub>. The recorded diffraction peaks could be assigned to M-

phase VO<sub>2</sub> (JCPDS card no. 82-0661, P21/c, a=0.575nm, b= 0.453nm, c=0.538nm). However, V<sub>3</sub>O<sub>7</sub> impurity peaks (JCPDS card no.71-1591) are detected. The (110) peak intensity first increase with W content increasing from 0 % to 3 %, while when W content increases to 5 %, the (110) intensity decreases. The plot of grain size as function of W concentration in fig. 4(b) also shows an obvious decrease trend, indicating the gradual expansion of VO<sub>2</sub> crystal lattice after W doped, thus inhibiting VO<sub>2</sub> grain growth.

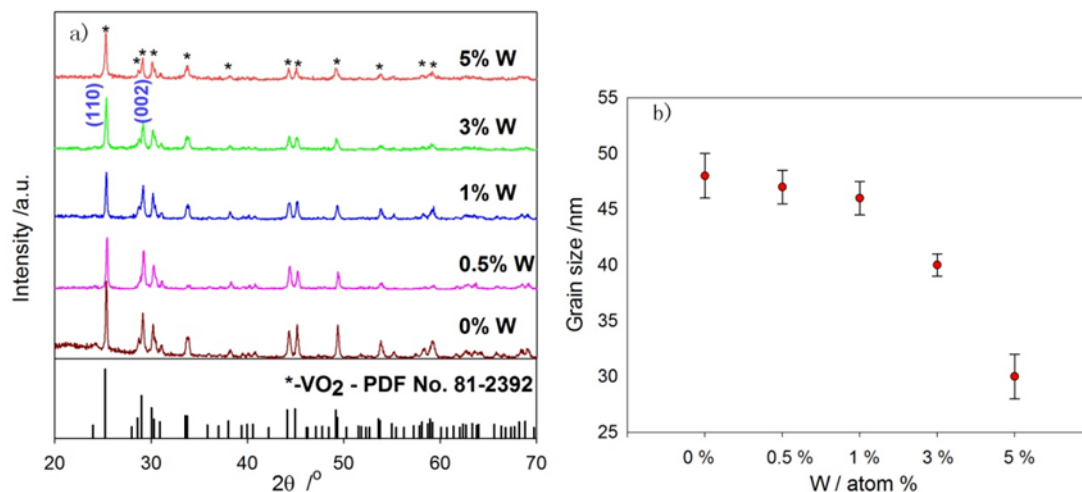


**Figure 4.** Fig. 4 XRD patterns and grain size analysis of annealed W-doped VO<sub>2</sub> powder: (a) The XRD patterns of obtained W-doped VO<sub>2</sub> (M) powder and (b) The plot of grain size as function of W concentration for W-doped VO<sub>2</sub> (M) powder.

#### 4. CONCLUSION

In this paper, both W-doped and undoped monoclinic VO<sub>2</sub> (B) powder were synthesized by hydrothermal process. The pure VO<sub>2</sub>(M) powder was obtained by heating dark blue VO<sub>2</sub>(B) at 750°C in nitrogen atmosphere for 2 h with granular VO<sub>2</sub>(M) with diameter around 1~2 microns. Wide W-doped concentrations VO<sub>2</sub> powders were also synthesized. The (110) peak of W-doped VO<sub>2</sub> (B) presented a tendency of shifting toward small reflection angle. V<sub>3</sub>O<sub>7</sub> phase was detected in W-doped VO<sub>2</sub> (M) samples, which suggested that subsequent annealing process and appropriate amount of WO<sub>2</sub>Cl<sub>2</sub> promoted the phase transition. Additionally, it was found that the diameter of W-doped VO<sub>2</sub> (M) particles was about micron level, larger than undoped VO<sub>2</sub> sample slightly. For W-doped VO<sub>2</sub> (M) samples, the grain size showed a steady decrease trend, as W-doped concentration increasing. In summary, a facile and available pathway was used to obtain VO<sub>2</sub> (M) powder, and there was potential use for VO<sub>2</sub> (M) production.

#### ACKNOWLEDGMENTS

This work is supported by the college natural science foundation (2013CJ29;R2013CJ08;M2014ME05). We appreciate Prof. Hongtao Zhang for theoretical instructions, Mr.Pu and Mrs.Teng for the XRD and SEM characterizations.

## References

1. F. Morin, *Phys. Rev. Lett.* 3 (1959) 34.
2. J.B. Goodenough, *J. Solid State Chem.* 3 (1971) 490.
3. W. Wang, B. Jiang, L. Hu, Z. Lin, J. Hou, S. Jiao, *J. Power Sources* 250 (2014) 181.
4. I. Mjejri, N. Etteyeb, F. Sediri, *Mater. Res. Bull.* 60 (2014) 97.
5. Z. Chen, Y. Gao, L. Kang, J. Du, Z. Zhang, H. Luo, H. Miao, G. Tan, *Sol. Energy Mater. Sol. Cells* 95 (2011) 2677.
6. J. Zhou, Y. Gao, Z. Zhang, H. Luo, C. Cao, Z. Chen, L. Dai, X. Liu, *Scientific Reports* 3 (2013).
7. I. Mjejri, N. Etteyeb, F. Sediri, *Ceram. Int.* 40 (2014) 1387.
8. M.J. Lee, Y. Park, D.S. Suh, E.H. Lee, S. Seo, D.C. Kim, R. Jung, B.S. Kang, S.E. Ahn, C.B. Lee, *Adv. Mater.* 19 (2007) 3919.
9. H. Zhang, Z. Wu, D. Yan, X. Xu, Y. Jiang, *Thin Solid Films* 552 (2014) 218.
10. J. Wu, W. Huang, Q. Shi, J. Cai, D. Zhao, Y. Zhang, J. Yan, *Appl. Surf. Sci.* 268 (2013) 556.
11. P. Kiri, M.E.A. Warwick, I. Ridley, R. Binions, *Thin Solid Films* 520 (2011) 1363.
12. A. Kaushal, N. Choudhary, N. Kaur, D. Kaur, *Appl. Surf. Sci.* 257 (2011) 8937.
13. L.H. Chen, C.M. Huang, J.H. Zhou, G. Xu, L. Miao, X.D. Xiao, *Advanced Materials Research* 463 (2012) 725.
14. Z. Peng, W. Jiang, H. Liu, *The Journal of Physical Chemistry C* 111 (2007) 1119.
15. Y. Zhang, J. Zhang, X. Zhang, Y. Deng, Y. Zhong, C. Huang, X. Liu, X. Liu, S. Mo, *Ceram. Int.* 39 (2013) 8363.
16. J. Zhou, Y. Gao, X. Liu, Z. Chen, L. Dai, C. Cao, H. Luo, M. Kanahira, C. Sun, L. Yan, *PCCP* 15 (2013) 7505.
17. W. Lv, D. Huang, Y. Chen, Q. Qiu, Z. Luo, *Ceram. Int.* 40 (2014) 12661.
18. S.R. Popuri, M. Miclau, A. Artemenko, C. Labrugere, A. Villesuzanne, M. Pollet, *Inorg. Chem.* 52 (2013) 4780.
19. L. Kang, Y. Gao, Z. Zhang, J. Du, C. Cao, Z. Chen, H. Luo, *Journal of Physical Chemistry C* 114 (2010) 1901.
20. Z. Zhang, Y. Gao, Z. Chen, J. Du, C. Cao, L. Kang, H. Luo, *Langmuir* 26 (2010) 10738.
21. X. Yang, X. Lian, S. Liu, G. Wang, C. Jiang, J. Tian, J. Chen, R. Wang, *Journal of Physics D-Applied Physics* 46 (2013).
22. J.M. Booth, P.S. Casey, *Phys. Rev. Lett.* 103 (2009).
23. M. Pan, H.M. Zhong, S.W. Wang, J. Liu, Z.F. Li, X.S. Chen, W. Lu, *J. Cryst. Growth* 265 (2004) 121.